Automatica 71 (2016) 254–263

Contents lists available at ScienceDirect

Automatica

journal homepage: www.elsevier.com/locate/automatica

Continuous-time identification of periodically parameter-varying state space models ☆

Jan Goos, Rik Pintelon

ELEC, Vrije Universiteit Brussel, Pleinlaan 2, 1050 Brussels, Belgium

ARTICLE INFO

Article history:
Received 17 November 2014
Received in revised form
22 March 2016
Accepted 1 April 2016
Available online 1 June 2016

Keywords:
Linear parametrically varying (LPV) methodologies
Experiment design
Identification methods

ABSTRACT

This paper presents a new frequency domain identification technique to estimate multivariate Linear Parameter-Varying (LPV) continuous-time state space models, where a periodic variation of the parameters is assumed or imposed. The main goal is to obtain an LPV state space model suitable for control, from a single parameter-varying experiment. Although most LPV controller synthesis tools require continuous time state space models, the identification of such models is new. The proposed identification method designs a periodic input signal, taking the periodicity of the parameter variation into account. We show that when an integer number of periods is observed for both the input and the scheduling, the state space model representation has a specific, sparse structure in the frequency domain, which is exploited to speed up the estimation procedure. A weighted non-linear least squares algorithm then minimizes the output error. Two initialization methods are explored to generate starting values. The first approach uses a Linear Time-Invariant (LTI) approximation. The second estimates a Linear Time-Variant (LTV) input–output differential equation, from which a corresponding state space realization is computed.

© 2016 Elsevier Ltd. All rights reserved.

1. Introduction

Although the Linear Time-Invariant framework (Pintelon & Schoukens, 2012) has given rise to powerful forms of control, the need to operate processes at even higher levels of precision requires more advanced model structures, like non-linear block structured models (Bai & Giri, 2010), time-varying differential equations (Lataire & Pintelon, 2011; Louarroudi, Lataire, Pintelon, Janssens, & Swevers, 2014), and Linear Parameter-Varying models (Rugh & Shamma, 2000; Tóth, 2010). Indeed, most physical systems behave non-linearly, or have a varying dynamic behavior that changes with an external parameter, like the temperature or pressure. Such systems are usually linearized at a chosen operating point. However, in practice it is quite common to utilize the same plant at several set points, each with their own linearized dynamics. A local LPV approach estimates LTI models at a set of operating points, after which a macro-model interpolates the local approximations (Bruzelius & Breitholtz, 2001; De Caigny, Camino, & Swevers, 2011; Ferranti, Knockaert, & Dhaene, 2011). These methods do not incorporate knowledge about the rate of variation of the scheduling parameter and, therefore, the resulting models are only valid in case of slow parameter variations. Contrary to the local approach, we opt for a global identification experiment (Rugh & Shamma, 2000), where the system dynamics are persistently changed by external signals $p(t)$, called the scheduling parameters. The goal is to identify the system from a single parameter-varying input–output experiment.

Modeling of arbitrary time-varying systems is challenging. In the identification phase, we will therefore focus on periodically parameter-varying systems. For example, the steady state operation of a rotating mechanical bearing (Allen, 2009) falls into this class. In other cases, where one has full control over the experimental setup, including the scheduling parameter $p(t)$, the periodicity can be imposed. In process applications, only a perturbation of the associated variables is allowed, due to limitations of actuation and process loss. In many cases, white noise, binary noise, PRBS or step inputs are used to perturb the system. It is also possible

☆ This work was supported in part by the Fund for Scientific Research (FWO-Vlaanderen), by the Flemish Government (Methusalem Fund, METH1), and by the Belgian Federal Government (IUAP VII, DYSCO). The material in this paper was presented at the 2014 American Control Conference, June 4–6, 2014, Portland, OR, USA and at the 53rd IEEE Conference on Decision and Control, December 15–17, 2014, Los Angeles, CA, USA. This paper was recommended for publication in revised form by Associate Editor Brett Ninness under the direction of Editor Torsten Söderström.

E-mail addresses: jan.goos@vub.ac.be (J. Goos), rik.pintelon@vub.ac.be (R. Pintelon).

http://dx.doi.org/10.1016/j.automatica.2016.04.013
0005-1098/© 2016 Elsevier Ltd. All rights reserved.

to use a random phase multisine excitation, resulting in a periodic experiment.

$$\sum_{k=\underline{K}}^{\overline{K}} A_k \cos(2\pi k f_0 t + \psi_k). \tag{1}$$

Here, A_k are user-defined, and ψ_k is uniformly distributed between $[0, 2\pi]$. Alternatively, the amplitudes and phases can be chosen, so that the system trajectory domain is explored optimally. In practice, a random phase multisine signal (1) cannot be discerned from a periodic white noise sequence in the time domain.

1.1. Target application

Most LPV controllers are designed in continuous time, using state space models (Apkarian & Gahinet, 1995; Scherer, 1996; Wu & Dong, 2006), which are given by

$$\dot{x}(t) = A\big(p(t)\big)x(t) + B\big(p(t)\big)u(t) \tag{2}$$

$$y_0(t) = C\big(p(t)\big)x(t) + D\big(p(t)\big)u(t)\,. \tag{3}$$

We define N_x as the size of the state vector $x(t)$ and denote the number of inputs $u(t)$, outputs $y(t)$ and scheduling signals $p(t)$ by N_u, N_y and N_p, respectively. For control design, ideally the coefficients depend only on the instantaneous value of the scheduling, i.e. linear combinations of known/chosen static basis functions in $p(t)$

$$A\big(p(t)\big) = \sum_{i=1}^{N_p} A_i\, \phi_i\big(p(t)\big) \tag{4}$$

where the matrices A_i are constant. A common choice for ϕ_i are the (multivariate) polynomials $p(t)^i$. Similar definitions hold for $B\big(p(t)\big)$, $C\big(p(t)\big)$ and $D\big(p(t)\big)$. The educated guess in the choice of basis function ϕ_i usually follows from the physics of the problem. In practice, the true coefficients will have to be approximated with the proposed basis in $\phi_i\big(p(t)\big)$. In Laurain, Tóth, Zheng, and Gilson (2012), Least Squares Support Vector Machines (LSSVM) are used, while in De Caigny et al. (2011) a polynomial basis is selected. From hereon, we call the collective set of (unknown) observed functions of the scheduling signals $p(t)$.

1.2. Existing work

Since we are essentially solving a non-linear optimization problem, the initial values for the parameters have a big impact on the results. In a first draft of the proposed identification approach (Goos, Lataire, & Pintelon, 2014), an LTI approximation was used, as illustrated in Fig. 1. The results were satisfactory, but when the parameter variation becomes larger or faster, the risk to end up in a local minimum increases. A simple time-invariant model can only approximate a slowly time-varying system. Therefore, in this paper we also examine another initialization routine, which is based on time-varying differential equations. Nowadays, a lot of research is dedicated to the identification of time- (Lataire & Pintelon, 2011; Louarroudi et al., 2014) and parameter-varying (Laurain, Tóth, Gilson, & Garnier, 2010; Tóth, Laurain, Gilson, & Garnier, 2012) differential equations.

$$\sum_{i=1}^{N_a} a_i(t)\, y^{(i)}(t) = \sum_{i=1}^{N_b} b_i(t)\, u^{(i)}(t) \tag{5}$$

$$\sum_{i=1}^{N_a} a_i(p(t)) y^{(i)}(t) = \sum_{i=1}^{N_b} b_i(p(t)) u^{(i)}(t)\,. \tag{6}$$

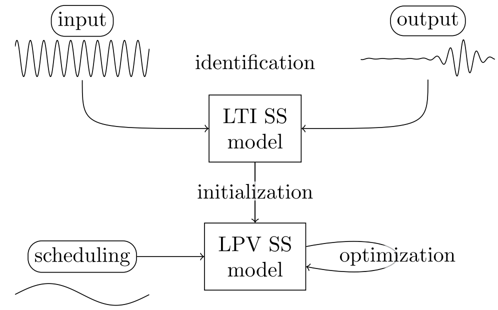

Fig. 1. Originally, the LPV identification was initialized with an LTI approximation. All coefficients related to the parameter variations are set to zero. The optimization searches for a good model, by minimizing the prediction error.

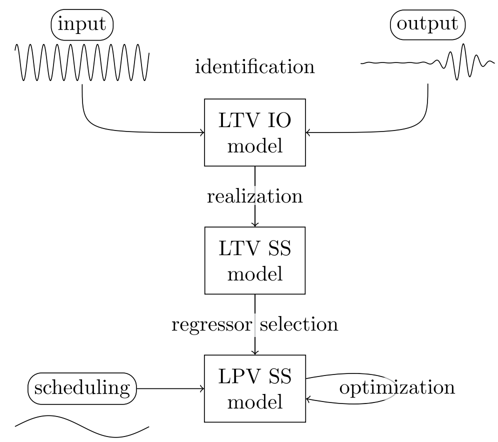

Fig. 2. First a general time-varying input–output model is identified. The corresponding minimal state space model is realized, with a dynamic dependence on the coefficients. Next, we try to establish a link between the known parameter variation $p(t)$ and the time-varying coefficients. Finally, the prediction error is minimized.

From Tóth (2010), we know that it is possible to transform a static parameter-varying differential equation into a minimal state space form, but the resulting models will have a dynamic dependence on the scheduling. From a control perspective, we want a simple, static model, in which the model only depends on the current value of $p(t)$. Therefore, direct application of Tóth (2010) does not yield the desired result.

Recently, we have derived exact computational formulas in the SISO case, to transform arbitrary (but smooth) time-varying differential equations like (5) into their minimal controllability canonical state space from Goos and Pintelon (2016). The formulas are given explicitly in Section 4, rather than implicitly, like in Tóth (2010), and can also be applied to LPV differential equations like (6). As in Tóth (2010), we find that, in general, a minimal realization introduces dynamic dependence on the scheduling variable $p(t)$. Although it is not guaranteed that a static minimal state space model exists, we can start the optimization routine (Goos et al., 2014) from the obtained model. Proceeding in this way, a simple, static model approximation can be fitted.

Specifically, in a first step we will use the Linear Periodic Time-Varying (LPTV) IO identification method described in Section 3.4, and realize a corresponding LTV SS model in Section 4. Next, Section 5 establishes a link between this time-varying state space model and basis functions of the scheduling parameter $f\big(p(t)\big)$. In a final step, we optimize the model fit using simple basis functions that are suitable for control design. The complete workflow is depicted in Fig. 2. Section 6 illustrates the proposed approach on a simulation example, and discusses the properties of all modeling steps.

1.3. Goal and contributions

The main goal of this research is to identify a continuous-time parameter-varying state space model from a single experiment, using a periodic scheduling and a periodic input. Summarized, the contributions of this paper are the following:

- the computationally efficient frequency domain calculation of the LPV state space equations.
- the construction of a frequency domain weighted non-linear least squares estimator for continuous time LPV state space equations.
- the generation of improved starting values.
- the reduction of the CT LPV SS equations to a control relevant form.

We want to stress that, once we have identified a model in the periodic setting, it is also valid for non-periodic inputs and scheduling trajectories. However, it is very ill-advised to use the model outside of the identified region, both for input and scheduling signals. As in the LTI identification framework, the experiment should match the operational conditions as close as possible.

2. An LPV SS model for control

This section details the LPV model construction in the frequency domain. We start by describing the assumptions on the measured signals and the measurement setup. Next, the state space equations are transformed into the frequency domain, where we show the sparse structure. These theoretical properties are used extensively in Section 3.2. Depending on the experimental conditions, not all assumptions are needed.

Assumption 1. The input $u(t)$ and the scheduling parameter $p(t)$ are synchronized periodic signals: $u(t+T_u) = u(t)$, $p\big(t+T_p\big) = p(t)$, and $T_u/T_p \in \mathbb{Q}^+$.

Assumption 2. The periodic steady-state response of the LPV system is observed.

Fact 3. *Under Assumptions 1 and 2, the response of an LPV system is periodic with a period T_y that is the least common multiple of T_u and T_p: $T_y = \text{lcm}(T_u, T_p)$.*

Assumptions 1 and 2 allow the use of well-established frequency domain identification techniques, for time-varying differential equations (Louarroudi et al., 2014) and parameter-varying state space models (Goos et al., 2014), without leakage and transient problems. Once identified, the LPV model is valid for non-periodic parameter variations and non-periodic inputs as well.

Assumption 4. The input $u(t)$ and the scheduling parameter $p(t)$ are known exactly, and noisy observations $y(t)$ of the output are available: $y(t) = y_0(t) + e_y(t)$ with $y_0(t)$ the true unknown value and $e_y(t)$ filtered (band-limited) white noise with finite mth order moments. The noise source $e_y(t)$ is assumed to be additive, and independent of the input $u(t)$.

Fact 3 is generally true only if $p(t)$ does not depend on the states $x(t)$. In the latter case, the underlying system is in fact nonlinear. It is possible to embed nonlinear systems in an LPV framework, but doing so requires additional assumptions, e.g. the steady state response to a periodic input is periodic with the same period as the input, also known as the Periodic Input, Same Periodic Output (PISPO) Assumption. Additionally, Assumption 4 requires $p(t)$ to be known exactly. This would mean that the states defining $p(t)$ have to be measured precisely.

In practice, the signals are synchronized if the generator and data acquisition clocks originate from the same mother clock. This is the case if the same device incorporates the generator and acquisition channels. If the generator and the measurement device are separated, the clock sync of the generator can be used as an input for the data acquisition clock. Additionally, to synchronize the periods, the input period T_u has to be chosen as a function of the scheduling period T_p, whether it is fixed or can be controlled.

Synchronized signals can be transformed to the frequency domain without introducing leakage errors (Pintelon & Schoukens, 2012), by means of the N-point Discrete Fourier Transform (DFT), with N the number of data samples. We call $f_0 = f_s/N$ the base frequency of the measurements, and $f_k = kf_s/N$ the DFT frequencies, where $k = -\frac{N}{2}+1, \ldots, \frac{N}{2}$ denotes the DFT bin number. Finally, we define the discrete Fourier transformed signals of $u(t)$, $p(t)$ and $y(t)$ as $U(k)$, $P(k)$ and $Y(k)$.

$$X(k) = \text{DFT}\left\{x(nT_s)\right\} = \sum_{n=0}^{N-1} x(nT_s)\, e^{\frac{-2\pi jkn}{N}} . \tag{7}$$

Assumption 5. The measurement setup is band-limited: the signals are lowpass filtered before sampling, and the input $u(t)$ and the scheduling parameter $p(t)$ are band-limited: $|U(k)| = 0$ and $|P(k)| = 0$ for $kf_0 \geq f_s/2$.

Assumption 6. The output error $e_y(t)$ is normally distributed, and uncorrelated with the true output signal.

Assumption 7. $M > N_y+2$ consecutive periods of the steady state response are measured.

2.1. The structured LPV identification problem

The additive structure from (4) can also be transformed into the frequency domain. The coefficient matrices A_i are constant, and the Fourier transform is a linear operator. Therefore, the multiplication $A_i\, p_i(t)$ in the time domain remains as a multiplication in the frequency domain. We denote the spectrum of the ith scheduling function by $P_i(k) = \text{DFT}\left\{\phi_i\big(p(t)\big)\right\}$. In the frequency domain, (4) then becomes

$$A\big(P(k)\big) = \sum_{i=1}^{N_p} A_i\, P_i(k) . \tag{8}$$

Note that simulating a dynamic system requires different computation methods in the time domain for the discrete and the continuous case. In the frequency domain, we only need to change the transformation variable, corresponding to the Z-transform $z = e^{j\omega T_s}$ or the Laplace transform $s = j\omega$, as in Chapter 7 of Pintelon and Schoukens (2012). Here, $T_s = 1/f_s$ is the sampling time. The drawback is that for the frequency domain approach, in both cases the measurements should be performed in steady state. In future research, we aim to relax this condition.

2.2. State space in the frequency domain

Similar to Goos et al. (2014), the continuous-time state space equations (2)–(3) can be converted to the frequency domain. Under Assumptions 1, 2 and 5, we find

$$j\omega_k X(k) = A\big(P(k)\big) * X(k) + B\big(P(k)\big) * U(k) \tag{9}$$

$$Y(k) = C\big(P(k)\big) * X(k) + D\big(P(k)\big) * U(k) . \tag{10}$$

$X(k)$, $U(k)$, $P(k)$, $Y(k)$ are the DFT transforms (7) of the state $x(t)$, the input $u(t)$, scheduling $p(t)$ and output $y(t)$ signals, respectively, and $*$ equals the circular convolution product of the spectra. In the LTI case, the $A(t)$, $B(t)$, $C(t)$ and $D(t)$ matrices are constant, and the convolution reduces to a regular multiplication.

Following Assumptions 2 and 5, the derivatives $\dot{x}(t)$ in (2) can be computed exactly in the frequency domain, as opposed to a discretized approximation, like in Laurain et al. (2010) and Tóth et al. (2012).

2.3. Band structure and sparsity

We can now impose the parametrization (4) on the state space equations (9)–(10). Recall that N data points are used, observed at a sample frequency f_s. We call $N_{P_p} = f_p/f_0$ the base bin of the time variation, meaning N_{P_p} periods of the time variation were measured. First, the circular convolution of two signals is written as a product of a Toeplitz matrix[1] and a vector:

$$P_i * X_i = \text{Toeplitz}\left(P_i, P_i^H\right) \times X_i \tag{11}$$

$$P_i = \begin{bmatrix} P_i(0) & \cdots & P_i\left(\frac{N}{2}\right) & P_i\left(-\frac{N}{2}+1\right) & \cdots & P_i(-1) \end{bmatrix}^T$$

$$X_i = \begin{bmatrix} X_i(0) & \cdots & X_i\left(\frac{N}{2}\right) & X_i\left(-\frac{N}{2}+1\right) & \cdots & X_i(-1) \end{bmatrix}^T$$

$$X = \begin{bmatrix} X_1^T & X_2^T & \cdots & X_{N_x}^T \end{bmatrix}^T.$$

Because the signals are real in the time domain, the Fourier coefficients at the negative frequencies are the complex conjugate of their positive counterparts: $P(-i) = P^H(i)$.

Now, each scheduling spectrum should be convolved with each state and input spectrum. To this end, block matrices are constructed. Collecting Eqs. (9)–(10) for all DFT frequencies $j\omega_k = 2\pi jkf_s/N$ yields

$$EX = \alpha\, P_x\, X + \beta\, P_u\, U \tag{12}$$

$$Y(\theta) = \gamma\, P_x\, X + \delta\, P_u\, U \tag{13}$$

where $U \in \mathbb{C}^{N_u N\times 1}$, $X \in \mathbb{C}^{N_x N\times 1}$ and $Y \in \mathbb{C}^{N_y N\times 1}$ are vertically stacked vectors containing the (DFT) spectra of the input, state and output, and

$$E = I_{N_x} \otimes \text{jdiag}\left(\omega_0, \omega_1, \ldots, \omega_{\frac{N}{2}}, \omega_{-\frac{N}{2}+1}, \ldots, \omega_{-1}\right) \tag{14}$$

$$\alpha = \left[\ A_1 \otimes I_N \mid A_2 \otimes I_N \mid \ldots \mid A_{N_p} \otimes I_N\ \right] \tag{15}$$

$$\beta = \left[\ B_1 \otimes I_N \mid B_2 \otimes I_N \mid \ldots \mid B_{N_p} \otimes I_N\ \right] \tag{16}$$

$$\gamma = \left[\ C_1 \otimes I_N \mid C_2 \otimes I_N \mid \ldots \mid C_{N_p} \otimes I_N\ \right] \tag{17}$$

$$\delta = \left[\ D_1 \otimes I_N \mid D_2 \otimes I_N \mid \ldots \mid D_{N_p} \otimes I_N\ \right] \tag{18}$$

$$P_x = \begin{bmatrix} \text{Toeplitz}\left(P_1, P_1^H\right) \otimes I_{N_x} \\ \vdots \\ \text{Toeplitz}\left(P_{N_p}, P_{N_p}^H\right) \otimes I_{N_x} \end{bmatrix} \tag{19}$$

$$P_u = \begin{bmatrix} \text{Toeplitz}\left(P_1, P_1^H\right) \otimes I_{N_u} \\ \vdots \\ \text{Toeplitz}\left(P_{N_p}, P_{N_p}^H\right) \otimes I_{N_u} \end{bmatrix} \tag{20}$$

α, β, γ and δ comprise the dynamics of the system, in which A_i, B_i, C_i and D_i are the original real time-domain matrices in Eq. (4). I_N is an $(N \times N)$ identity matrix and $\otimes$ is the Kronecker product. From this compact notation, we can clearly see that the matrices are actually only defined by a limited number of parameters. These unknown matrix coefficients are collected in the model parameter vector $\theta \in \mathbb{R}^{(N_x+N_y)N_p(N_x+N_u)\times 1}$

$$\theta_i = \left[\text{vec}(A_i)^T, \text{vec}(B_i)^T, \text{vec}(C_i)^T, \text{vec}(D_i)^T\right]^T \tag{21}$$

$$\theta = \left[\theta_1^T, \theta_2^T, \ldots, \theta_{N_p}^T\right]^T \tag{22}$$

which is to be identified. Note that θ is a constant, real vector. The parameter variation enters the frequency domain model (12)–(13) via the spectra P_i of the basis functions $\phi_i\big(p(t)\big)$. Contrary to the LTI case, all equations are coupled, and must therefore be solved together. Nonetheless, the inherent Toeplitz structure can be used to speed up the calculations.

Assumption 8. The scheduling signals are varying slowly, meaning the frequency content of $P(k)$ is only non-zero in a limited range with respect to the frequency band of interest. Recall from (1) that the highest excited input frequency is $\overline{K}f_0$. Therefore,

$$\begin{cases} \|P(k)\|_0 \neq 0 & kf_0 \ll \overline{K}f_0 \\ \|P(k)\|_0 = 0 & \text{else.} \end{cases}$$

If the parameter variation is slowly varying with respect to the excited frequency band, the frequency domain state space representation (12)–(13) becomes sparse. The block Toeplitz matrices P_x and P_u then become sparse block band matrices. For example, if the matrix coefficients vary with a single sine around a mean value, only $P_2(-1)$, $P_1(0)$ and $P_2(1)$ are non-zero. Similarly, if multiple (N_{T_p}) periods of the scheduling are observed, only the N_{T_p}th off-diagonals are non-zero.

Eqs. (12)–(13) still hold for scheduling signals with a larger bandwidth, e.g. similar to that of the input signal, but then the sparsity is lost, and the computations become less computationally efficient. Worse, Section 3.3 will show that a time-invariant initialization scheme, shown in Fig. 1, will suffer from scheduling signals that are varying too fast. For the initialization with the time-varying model, depicted in Fig. 2, a slightly different assumption is formulated:

Assumption 9. The scheduling signals have a limited number of frequency components. The parameter variation does not need to be slow, but it should be band-limited, as stated in Assumption 5.

$$\sum_k \|P(k)\|_0 \ll N.$$

The sum over the zero-norm of the scheduling spectrum should be small with respect to the number of data points, for reasons of identifiability. Suffice to say that Assumption 9 is a bit more general than Assumption 8.

Note that, if the convolution $P_i * U$ or $P_i * X$ creates spectral content outside the measurable frequency band $kf_0 > f_s/2$, it is eliminated by the anti-alias filters in the band-limited setup of Assumption 5. This information is lost, and cannot be used for identification. Caution is advised in the lower frequency range as well. There, energy can end up in the negative frequencies, which is not filtered. By considering the circular convolution, as stated in Section 2.2, these aliasing effects can be modeled. Nevertheless, Eqs. (12)–(13) simplify when the spectrum of the output Y has a margin with respect to DC and the Nyquist frequency.

3. Non-linear optimization routine: minimizing the weighted output error

In order to identify the matrix coefficients that define the dynamics, the weighted output error is chosen as the optimization criterion, and the Gaussian Maximum Likelihood Estimator is

1 www.mathworks.com/help/matlab/ref/toeplitz.html.

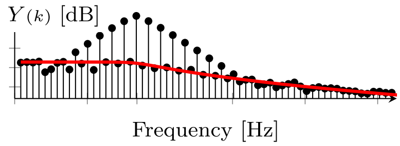

Fig. 3. Output spectrum $Y(k)$ of a periodic parameter-varying system for a single sine excitation. Energy appears only at the harmonic frequencies. If multiple periods are measured, a non-parametric noise model (-) can be estimated.

formulated in the frequency domain. For a given model with parameters θ, the output error is defined as the difference between the DFT spectra of the modeled $Y(\theta)$ and the measured output Y:

$$\varepsilon(\theta) = Y(\theta) - Y. \tag{23}$$

Under Assumptions 1, 2 and 4–6, the Gaussian MLE $\hat{\theta}_{\mathrm{ML}}$ minimizes the following cost function, given the data Z:

$$V_{\mathrm{ML}}(\theta, Z) = \varepsilon(\theta)^H\, C_e^{-1}\varepsilon(\theta) \tag{24}$$

$$\hat{\theta}_{\mathrm{ML}} = \underset{\theta}{\operatorname{argmin}}\; V_{\mathrm{ML}}(\theta, Z) \tag{25}$$

with C_e the error covariance matrix. The latter can be estimated non-parametrically in the frequency domain, by simply observing multiple periods of the output signal (Mahata, Pintelon, & Schoukens, 2006; Pintelon, Vandersteen, Schoukens, & Rolain, 2011), as illustrated by Fig. 3. As stated in Assumption 4, only stationary output noise is considered here. Hence, the noise is uncorrelated over the frequency, and C_e becomes a (non-constant) block diagonal matrix (the noise can still be correlated over the N_y outputs).

If a controller is needed to ensure the periodic motion of the system, due to losses and disturbances, the (controlled) input becomes noisy as well. Appendix discusses how the error covariance matrix can be computed in the case of input noise. The proposed identification method then effectively becomes an Errors-In-Variables scheme, like (Tóth et al., 2012).

If only a limited frequency band is of interest, the ML cost function can easily be adapted. Suppose that a high sample frequency f_s is used, but the dynamics are dominant at lower frequencies. Then, we want to fit the output spectrum, by selecting the entries of ε lying in the low frequency region only. Note, however, that the computation of $Y(\theta)$ requires all frequencies.

3.1. The minimization algorithm

To solve the non-linear optimization problem of the MLE cost function, an iterative Gauss–Newton method is employed. It has the advantage that only the Jacobian of the output errors is calculated, which greatly benefits from the computationally efficient model response calculation discussed in Section 2.3. For details, we refer to Chapter 9.4 in Pintelon and Schoukens (2012).

We know from the literature (Goos & Pintelon, 2016) that a state space representation is only determined up to a similarity transformation. The Jacobian will therefore be singular: its rank is equal to the effective number of parameters. Nevertheless, because we know the rank on beforehand, the pseudo-inverse can be used to find an update for the model parameters in a numerically stable way (Wills & Ninness, 2008).

Assumption 10. Persistency of excitation and scheduling condition: the rank of the Jacobian matrix should be $(N_x + N_u)N_p(N_x + N_x) - N_x^2$, which is the number of effective parameters.

The proposed basis functions $\phi_i\big(p(t)\big)$ indirectly impose a spectral richness condition on the scheduling $P(k)$. If the number of scheduling functions N_p increases, the original scheduling signal has to excite more frequencies.

Example 11. A single sine is applied as a scheduling $p(t) = \sin(\omega t)$, but we need to identify the coefficient of $\ddot{p}(t) = -\omega^2 \sin(\omega t)$. It is impossible to discern p and $\ddot{p}$ by using a single frequency ω.

3.2. Statistical properties of the minimization problem

The maximum likelihood estimator has great statistical properties, because of the "optimal" weighting of the output error. Measurements with a lot of variance are uncertain, and should therefore not be fitted so strictly. The following theorems study the weighted non-linear least squares (WNLS) estimator (25) when the number of excited input frequencies $F = \mathcal{O}(N)$ tends to infinity.

Assumption 12. The true model is in the model class (12)–(13), covering the dynamical order N_x of the system, and the proposed basis functions $\phi_i\big(p(t)\big)$.

Theorem 13. *Under Assumptions 1, 2 and 4 ($m = 4$), 5, 10 and 12, the WNLS estimator (25) is consistent. If in addition Assumption 4 ($m = \infty$) holds, then (25) is asymptotically normally distributed. If Assumption 6 is also fulfilled, then (25) is the Gaussian MLE and it is asymptotically efficient.*

The consistency proof is based on the key property that the expected value of (24) is minimal in the true model parameters θ_0. The rest of the proof follows the same lines of Theorem 9.21 in Pintelon and Schoukens (2012). Theorem 13 can be used if the error covariance matrix is known beforehand. Otherwise, C_e has to be estimated from the data. In this case, we also need $e_y(t)$ to be normally distributed (Assumption 6) to prove consistency.

Theorem 14. *If C_e is estimated from M consecutive periods (Assumption 7), then under Assumptions 1, 2* and *4–6*

$$\hat{\theta}_{\mathrm{SML}} = \underset{\theta}{\operatorname{argmin}}\; \varepsilon(\theta)^H\, \hat{C}_e^{-1}\varepsilon(\theta) \tag{26}$$

is consistent and asymptotically normally distributed with asymptotic covariance

$$\operatorname{Cov}(\hat{\theta}_{\mathrm{SML}}) = \frac{M - N_y - 1}{M - N_y - 2}\operatorname{Cov}(\hat{\theta}_{\mathrm{ML}}). \tag{27}$$

The proof follows the same lines of Mahata et al. (2006).

3.3. Generating simple starting values: the best linear approximation

In the first draft of the proposed optimization scheme (Goos et al., 2014), the Best Linear Time-Invariant or BLTI approximation (Lataire, Louarroudi, & Pintelon, 2012; Pintelon, Louarroudi, & Lataire, 2012) was used. Basically, an LTI model tries to fit only the output frequencies f_u that were excited by a random phase multisine (1) at the input. The slower and the smaller the parameter variation, the better the BLTI model will approximate the underlying system.

Now, for slowly varying systems, it is possible to obtain estimates for all the B_i and D_i, instead of only the time-invariant parts B_1 and D_1. Following the same lines of Lee and Poolla (1999), the input $u(t)$ can be virtually expanded with parameter-varying $\phi_i\big(p(t)\big)u(t)$, because the scheduling is assumed to be known. The resulting MISO or MIMO system can be modeled by any LTI identification method. The optimization routine then tries to fill in the blanks. The resulting two-step procedure is illustrated by the flowchart in Fig. 1.

3.4. Initialization via time-varying differential equations in the frequency domain

Alternative to Section 3.3, we propose an indirect initialization method, using the Linear Time-Varying (LTV) framework in the frequency domain (see Fig. 2). The time-varying coefficients $a_i(t)$ and $b_i(t)$ in (5) can be seen as a realization for a particular scheduling signal $p(t)$. Indeed, each trajectory of $p(t)$ corresponds with its own LTV model. However, a reverse link exists as well. By first identifying an LTV model with more degrees of freedom, it is possible to extract some preliminary knowledge about the underlying system. The link with LPV modeling will be discussed in more detail in the sequel. Due to space limitations, we will not discuss the details of the identification technique for LTV differential equations with a periodic time variation. The interested reader is referred to Louarroudi et al. (2014). We will simply state that the input–output equation is structured and sparse in the frequency domain. Furthermore, the LTV IO estimator (Louarroudi et al., 2014) is consistent, and can easily be initialized with a Linear least Squares (LS) estimator.

4. Canonical LTV state space realization

The second step in the indirect initialization method of Fig. 2 entails the state space realization of the identified time-varying differential equation. To this end, we introduce a closed form SS expression, for which the proof is given in Goos and Pintelon (2016). For a general proper input–output model, the corresponding companion observability canonical form, or phase-variable observability form or just simply "observable" canonical form, is given by

$$\dot{x} = \begin{bmatrix} 0 & \cdots & 0 & \frac{\alpha_0}{a_n} \\ 1 & \cdots & 0 & \frac{\alpha_1}{a_n} \\ \vdots & \ddots & \vdots & \vdots \\ 0 & \cdots & 1 & \frac{\alpha_{n-1}}{a_n} \end{bmatrix} x + \begin{bmatrix} \frac{\beta_0}{a_n} \\ \frac{\beta_1}{a_n} \\ \vdots \\ \frac{\beta_{n-1}}{a_n} \end{bmatrix} u \tag{28}$$

$$y = \begin{bmatrix} 0 & 0 & \cdots & \frac{1}{a_n} \end{bmatrix} x + \begin{bmatrix} \frac{b_n}{a_n} \end{bmatrix} u \tag{29}$$

where

$$\alpha_r = \sum_{i=r}^{n} (-1)^{i-(r+1)} C_i^r a_i^{(i-r)} \tag{30}$$

$$\beta_r = b_n \sum_{i=r}^{n} (-1)^{i-(r+1)} C_i^r a_i^{(i-r)} - a_n \sum_{i=r}^{n} (-1)^{i-(r+1)} C_i^r b_i^{(i-r)}. \tag{31}$$

The time dependence of the coefficients was omitted to avoid cluttering the equations. We denote $a^{(i)}$ as the ith derivative of a. The order of the model is $n = N_x = N_y N_a$, and we have the binomial coefficients

$$C_i^k = \frac{i!}{(i-k)!k!} = \binom{i}{k}. \tag{32}$$

As in the LTI case, the expression simplifies when the system is proper $N_a > N_b$, because then $b_n = 0$.

Remark 15. The proposed time-varying state space realization is minimal in the single output case, but requires derivatives of the coefficient functions $a_i(t)$ and $b_i(t)$ of the differential equation (5). When applied to an LPV differential equation, this corresponds with a dynamic dependence on the scheduling variable $p(t)$. Although the transformation holds for arbitrary time-varying systems, the higher order derivatives $a_i^{(i)}$ up to order i must exist.

Remark 16. Note that in the periodic band-limited setup of Assumptions 1 and 5, the derivatives can be computed exactly in the frequency domain. The state space realization step is therefore also exact.

Assumption 17. For the observability canonical form, the highest order term $a_n(t)$ should not become zero $\forall t$.

An alternative state space realization approach (33)–(34) is given in Wiberg (1971) on pages 25–26, assuming $a_n(t) = 1$. It has the interesting property that the A matrix has been made time-invariant, at the cost of increasing the complexity of the B matrix. Both representations are equivalent, and by means of the possibly time-varying similarity transformations an infinite number of alternatives are possible. In the sequel, we will discuss the possible advantages of both realization schemes.

$$\dot{x} = \begin{bmatrix} 0 & 1 & \cdots & 0 \\ \vdots & \ddots & \ddots & \vdots \\ 0 & 0 & \cdots & 1 \\ -a_0 & -a_1 & \cdots & -a_{n-1} \end{bmatrix} x + \begin{bmatrix} \gamma_{n-1} \\ \vdots \\ \gamma_1 \\ \gamma_0 \end{bmatrix} u \tag{33}$$

$$y = \begin{bmatrix} 1 & 0 & \cdots & 0 \end{bmatrix} x + \begin{bmatrix} \gamma_n \end{bmatrix} u \tag{34}$$

where

$$\gamma_n = b_n \tag{35}$$
$$\gamma_{n-i} = b_{n-i} - \sum_{k=0}^{i-1} \sum_{j=0}^{i-k} C_{n-i+j}^{j} a_{n-i+j+k}(t) \frac{d^j \gamma_{n-k}(t)}{dt^j}.$$

Eq. (35) shows that the second LPV realization requires combinations of powers and derivatives of the coefficient functions a_i and b_j, which introduces more basis functions for the exact SS form. From this point of view, the first canonical form (28)–(29) performs better. However, in some cases (33)–(34) immediately allows for a static minimal state space representation.

Assumption 18. The right hand side coefficients in (5) are constant $b_i(t) = \overline{b_i}\ \forall i > 0$.

Assumption 19. Given a threshold index $N_{\text{var}} < N_a$, the right hand side coefficients are zero $b_i(t) = 0\ \forall i > N_{\text{var}}$. Additionally, the corresponding left hand side coefficients are constant $a_i(t) = \overline{a_i}\ \forall i > N_{\text{var}}$.

Theorem 20. *Under Assumptions 18 and 19 the state space realization (33)–(34) does not require any derivatives of the coefficient functions $a_i(t)$ and $b_i(t)$.*

The transformation from a time-varying differential equation, with no derivatives of the input $b_{i>0}(t) = 0$, to a state space form is perhaps more generally known (Levine, 2011). However, the proposed realization schemes (28)–(29) and (33)–(34) are more general. In practice, the actuator might affect acceleration as well as the jerk. Then, derivatives of the input force $u(t)$ come into play, and the realization becomes more involved.

5. The link between the time-varying and parameter-varying model

The final step in the flowchart of Fig. 2 establishes the link between the identified time-varying input–output coefficients and the (known) scheduling signal, so we end up with a parameter-varying model. In Fig. 2, the time-varying differential equation (5) is first transformed into an LTV state space form, and then fitted with an LPV model. Alternatively, let us explore the transformation of a parameter-varying input–output equation (6), with polynomial coefficient functions of $p(t)$. We apply the chain rule of derivation, and find that

$$\tfrac{d}{dt}a_i(p(t)) = \tfrac{d}{dp}a_i(p(t))\,\tfrac{dp}{dt} \tag{36}$$

$$\tfrac{d^2}{dt^2}a_i(p(t)) = \tfrac{d^2}{dp^2}a_i(p(t))\,(\tfrac{dp}{dt})^2 + \tfrac{d}{dp}a_i(p(t))\,\tfrac{d^2p}{dt^2}. \tag{37}$$

The required basis functions for the state space realization are a mix of derivatives of the coefficients $a_i(p(t))$ and $b_i(p(t))$ with respect to $p(t)$, and the time derivatives of the scheduling parameter itself. If either of these components becomes small, the complete term becomes negligible with respect to the contributions of the static components. Therefore, the slower the parameter variation, the less impact the dynamic dependency has on the model. Now, from a control synthesis point of view, any dynamic dependence on the scheduling parameter is undesired. The following example illustrates why:

Example 21. Consider the case of (28)–(29) where $a_1(t) = 1 + p_1(t)^2$. The scheduling parameter is a single signal: $p(t) = p_1(t)$, and its time derivative equals $\dot{a}_1(t) = 2p_1(t)\,\dot{p}_1(t)$. Once the trajectory $p_1(t)$ is fixed, so is $\dot{a}_1(t)$. However, the latter depends dynamically on the scheduling, which cannot be taken into account by a static controller. Therefore, an additional "virtual" scheduling parameter $p_2(t) = p_1\dot{p}_1(t)$ would have to be defined, meaning the scheduling vector now has two components $p(t) = [p_1(t)\,,\, p_2(t)]^T$. Even though the coefficient functions lie on a specific curve, the controller would have to cover the worst-case scenario, and make sure that all possible combinations of $1+p_1(t)^2$ and $p_2(t) = p_1(t)\,\dot{p}_1(t)$ are stabilized, introducing unnecessary design constraints and conservativeness.

Although recent LPV controller synthesis tools based on Lyapunov theory can handle affine (Apkarian, Gahinet, & Becker, 1995), polynomial (Chesi, Garulli, Tesi, & Vicino, 2007) and even rational (Apkarian & Adams, 1998) parameter-dependent Lyapunov matrices, dynamic dependence is not considered. Simply put, a controller with a less complex parameter dependency is easier to synthesize, and simpler to implement. Therefore, we aim for a static LPV state space model, with polynomial basis functions $\phi_i\big(p(t)\big) = p(t)^i$. Generally, any static, smooth functions $a(p(t))$ and $b(p(t))$ can be approximated arbitrarily well over the finite interval $[p_-, p_+]$ by a polynomial basis in p, so this assumption does not pose a problem.

5.1. Exact static state space realization

Given a periodic time-varying differential equation (5), it is possible to plot the coefficient functions with respect to the scheduling vector. Proceeding in this way, we can get an idea of which basis functions to use. If the resulting graph does not look like a static function, a dynamic dependence on the scheduling is needed. Note that this intuitive, graphic approach is limited in the case of multiple scheduling variables, because the relation between the scheduling vector $p(t)$ and the coefficients $\theta(t)$ becomes a multiple-input single-output function, that generally will be non-linear and dynamic, which is hard to visualize. However, once a set of basis functions $\phi_i\big(p(t)\big)$ is chosen, a (regularized) least squares approximation can be readily computed (for example using lasso), whether there are multiple scheduling variables or just a single one.

Let us briefly assume that the coefficient functions $a(p(t))$ and $b(p(t))$ of the LTV differential equation (5) can be fitted with polynomials $\phi_i\big(p(t)\big) = p(t)^i$ of an appropriate order. If Assumptions 18 and 19 hold, a minimal, static state space realization can be obtained via the transformation (33)–(34). Since the identification method (Louarroudi et al., 2014) is consistent, and the realization step is exact, no additional optimization is required.

5.2. Static state space approximation

It is possible that Assumptions 18 and 19 do not hold, or worse, that the fitting of the time-varying input–output equation already requires a dynamic mapping. In this case, we want to find a good static approximation of the true (dynamic) state space model, by fitting the realized time-varying state space model with static basis functions, using (regularized) least squares, or some kind of matrix norm.

If the time-varying differential equation does not meet Assumptions 18 and 19, neither one of the transformations (28)–(29) or (33)–(34) will result in a state space model that has a dynamic dependence on the scheduling. It is hard to predict which one will be "closer" to a static model.

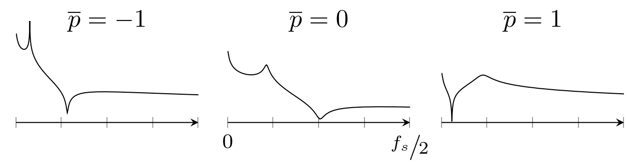

Fig. 4. Local LTI characteristics of the antiresonance system (38). Both the resonance and the antiresonance frequency shift considerably. Even more, the damping coefficients adapts as well.

6. Simulation example: the static state space approximation of a third order LPV system

To illustrate the properties of the proposed indirect identification method, we study a third order LPV system, with shifting resonance and antiresonance frequencies, as well as a parameter-varying damping. In this case study, the scheduling parameter ranges between −1 and 1. We take $N = 3000$ samples at a sampling rate of $f_s = 4.7747$ Hz, meaning the frequency resolution is $f_0 = f_s/N = 0.0016$ Hz. Fig. 4 shows some "frozen" LTI transfer functions, where the scheduling signal is kept constant $p(t) = \overline{p}$. From Fig. 4, it can be seen that the eigenfrequencies vary significantly with respect to the Nyquist frequency $f_s/2$, and the resonance and antiresonance even cross one another.

The following third order differential equation is obtained by interpolating a set of 21 frozen LTI input–output models, with a third order polynomial in $p(t)$:

$$\begin{aligned}
&(1+p^2)y^{(3)} \\
&\quad + (0.3289 + 0.5875p + 0.7903p^2 + 0.4260p^3)y^{(2)} \\
&\quad + (10.2539 + 10.2694p + 2.5970p^2 + 0.0213p^3)y^{(1)} \\
&\quad + (0.5120 + 0.5120p + 0.1280p^2)y \\
&= (0.0050 + 0.0400p^2)u^{(2)} + (0.0024 - 0.0016p)u^{(1)} \\
&\quad + (0.2880 - 0.3840p + 0.1280p^2)u.
\end{aligned} \tag{38}$$

This system is excited with a rich random phase multisine (see Fig. 5) and the scheduling is a random phase multisine (1) with

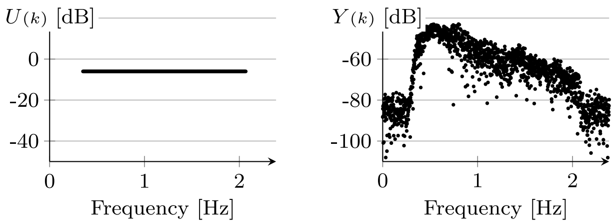

Fig. 5. Spectra (•) (in dB) for the LPV IO model (38), over the entire measurement record. (left) The input is a random phase multisine (1), which has a flat amplitude spectrum. (right) Corresponding output spectrum, for a scheduling signal ∈ [−1, 1] with 20 harmonic frequencies.

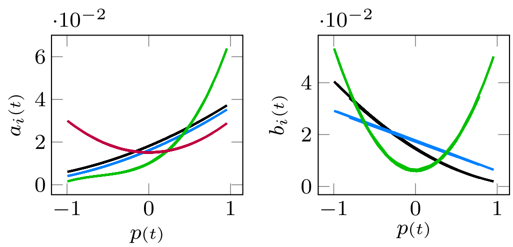

Fig. 6. Normalized time-varying coefficients $a_i(t)$ and $b_i(t)$, with respect to the scheduling signal $p(t)$. From these plots, we can deduce the polynomial order N_p, and verify that the differential equation can be modeled with static coefficients.

20 harmonic components ($\overline{K} = 1$, $\underline{K} = 20$) where the amplitudes A_k are chosen such that $\max |p(t)| = 1$. The periodic steady state response is measured with white output noise of 30 dB SNR. Fig. 5 shows the noisy output spectrum (•).

The LTV identification method (Louarroudi et al., 2014) is consistent, and we obtain a very good estimate of the time-varying differential equation (38), given the trajectory $p(t)$. The plots in Fig. 6 correspond with the true differential equation (38). Since the scheduling signal is one-dimensional, the identified time-varying coefficients can be plotted as a function of $p(t)$. This allows us to verify that the differential equation is static with respect to the scheduling, and it can be modeled with a polynomial basis of order 3 and 2 for $a_i(t)$ and $b_i(t)$, respectively.

As indicated in Louarroudi et al. (2014), the limitation of the LTV approach lies in the number of estimated parameters. Each additional frequency of $p(t)$ that has to be estimated, is combined with the others via the polynomial nonlinearities. This results in $(N_a + 1)N_p + (N_b + 1)N_p$ additional complex model parameters. Note that it is possible to estimate a fast (but periodic) time-varying model. Given the scheduling frequencies and the chosen basis functions, only the required harmonics can be selected in the identification procedure, reducing the number of model parameters. Experiment design is therefore important.

Since the time-varying model does not meet Assumptions 18 and 19, we cannot find a static state space model using Theorem 20. Therefore, it is not necessary to relate the scheduling parameter and the time-varying coefficients yet. Instead, either one of the canonical forms (28)–(29) or (33)–(34) can be used on the LTV input–output model, to obtain an exact LTV state space model. Both methods will result in an LPV model with a dynamic dependence on $p(t)$.

Fig. 7 shows the nonlinear dynamic relation between the realized time-varying state space coefficients, using the transformation (33)–(34). The $A_{[i,j]}(p(t))$ functions are static, because the identified differential equation (38) is polynomial in $p(t)$. However, the $B_{[i,j]}(p(t))$ coefficients become more complex, and even require a dynamic mapping in the case of $B_{[2,1]}(p(t))$. Clearly, a static approximation with polynomial basis functions $\phi_i\big(p(t)\big) = p(t)^i$ cannot be exact. Nevertheless, the obtained LTV SS model is fitted by a

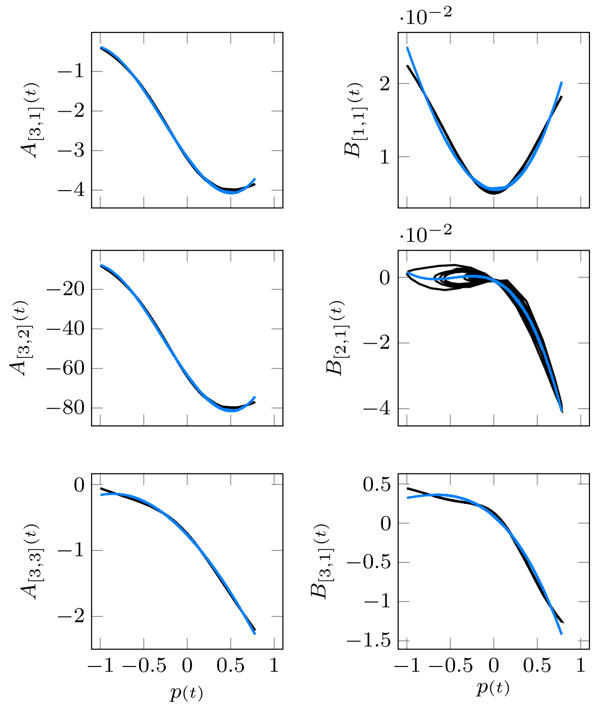

Fig. 7. Realized time-varying state space coefficients (–) $A_{[i,j]}(t)$ and $B_{[i,j]}(t)$, plotted against the scheduling signal $p(t)$. The static parameter-varying coefficients, obtained via least squares regression with a polynomial basis functions $\phi_i\big(p(t)\big) = p(t)^i$ are shown on top (–).

simple least squares regression, to serve as initial estimate for the optimization routine of Section 3.

Fig. 8 shows the output spectrum (•) and the model error (•), for the initial static approximation. Although the error is an order of magnitude smaller then the output, it is still far above the noise floor, which lies round −85 dB. After the optimization, which uses a full (polynomial) parametrization of the state space matrices, the residual drops down close to the noise level (▪). The model is not perfect, but it can approximate the parameter-varying input–output dynamics quite well, for the maximum scheduling frequency of 0.03183 Hz.

Fig. 9 plots the true output signal and the model error in the time domain, together with the scheduling trajectory used in the identification step. For small values of $p(t) \simeq -1$, a sharp resonance peak appears at low frequency, which is consistent with the frozen LTI snapshots in Fig. 4.

The original, direct state space identification method performs poorly in this example. Because the scheduling parameters is moving quite fast, the effect of the time variations start to affect the output spectrum at other excited lines. A simple LTI model just cannot grasp this complexity, and the initial fit will be poor, resulting in a large output error (•), even after the optimization. Indeed, a good initial estimate is paramount.

Fig. 10 shows the performance of the identified LPV state space model on a validation set. An independent random phase multisine was applied at the input, and the scheduling trajectory follows a triangle wave. Since the model is not exact, new data cannot be predicted exactly. To avoid overfitting, it is a good idea to supply the optimization routine with multiple datasets, if possible.

In summary, the identified approximate static LPV state space model explains the differential equation (38), with polynomial parameter variation, pretty well, even though an exact state space model would have required a dynamic dependence on the scheduling signal.

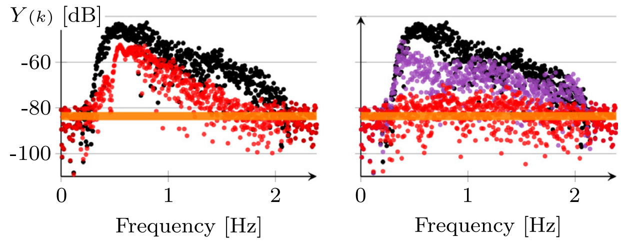

Fig. 8. (left) True output spectrum (•) of the initial static approximation, given the time-varying state space realization of (38). The error (•) lies far above the noise standard deviation (▬). (right) Optimized polynomial state space model. The error (•) of the indirect method is comparable with the noise level (▬). The error of the optimized BLTI model (•) cannot reach the noise floor.

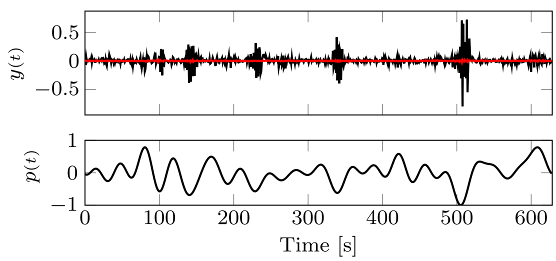

Fig. 9. True output (-) and scheduling signals (-) in the time domain. The prediction error of the polynomial state space model is shown in red (-).

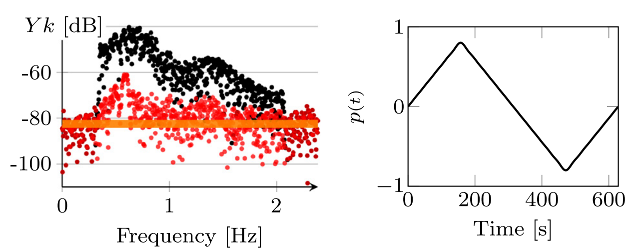

Fig. 10. (left) True output spectrum (•) and model error (•) of the estimated LPV state space model, for the triangular validation scheduling trajectory (right). The error increases a little w.r.t. Fig. 8, but the order of magnitude is still similar to the noise standard deviation (▬).

7. Conclusion

In this paper, we have given an overview of recent work on frequency domain modeling of parameter-varying state space models. If the time variation and the input are periodic and synchronized, we have shown that the resulting equations become structured and sparse in the frequency domain.

In a first attempt, the optimization routine started from the best linear time-invariant approximation. This approach works well when the parameter variation is slow and small with respect to the dynamics of the system. Alternatively, it is possible to extract a minimal canonical state space representation, via the well-established identification of a general periodic time-varying differential equation. However, the model coefficients then have a dynamic dependency on the scheduling, which is undesired for control design. Note that currently there is no proof that a static state space realization exists, let alone a minimal one. Through the general time-varying input–output model, we can visually inspect the relation between the obtained model coefficients and the scheduling signal. This gives us a qualitative measure for the influence of the scheduling dynamics.

Because the targeted application is LPV control, the emphasis was put on the identification of an LPV state space model which has a simple static relation with $p(t)$. By using only a polynomial basis in $p(t)$, we can already obtain a reasonable static approximation. Nevertheless, if the parameter variation becomes faster, fitting the time-varying state space coefficients with only static functions will result in a crude initialization. However, thanks to the over-parametrization of a state space model, we have not experienced convergence problems.

The proposed identification techniques were verified on a third order simulation example, with no exact static state space counterpart. In the presence of additive noise on the output, the proposed identification method is still able to obtain a decent approximate polynomial LPV SS model, as shown on an independent validation dataset.

In future research, we aim to relax the periodicity conditions on the input. The LTV identification method of Lataire and Pintelon (2011) can already handle non-periodic, noisy inputs and outputs. Recently, the state space identification method of Goos et al. (2014) was extended to handle arbitrary inputs as well (Goos, Lataire, & Pintelon, 2015). Therefore, the main idea of this paper should still be applicable.

Appendix. The error covariance matrix C_e in the presence of input noise

The definition of the output error follows from (12)–(13):

$$e = Y - \left[(E - \alpha\, P_x)^{-1}\beta + \delta\right] P_u\, U. \tag{A.1}$$

Subsequently, the output error covariance is given by

$$C_e(\theta) = \begin{bmatrix} I_N & -\mathbf{B} \end{bmatrix} \begin{bmatrix} C_Y & C_{YU} \\ C_{YU}^H & C_U \end{bmatrix} \begin{bmatrix} I_N \\ -\mathbf{B}^H \end{bmatrix} \tag{A.2}$$

with I_N an $(N \times N)$ identity matrix.

References

Allen, M. S. (2009). Frequency-domain identification of linear time-periodic systems using LTI techniques. *Journal of Computational and Nonlinear Dynamics*, *4*(4).

Apkarian, P., & Adams, R. J. (1998). Advanced gain-scheduling techniques for uncertain systems. *IEEE Transactions on Control Systems Technology*, *6*(1), 21–32.

Apkarian, P., & Gahinet, P. (1995). A convex characterization of gain-scheduled H_∞ controller. *IEEE Transactions on Automatic Control*, *40*(5), 853–864.

Apkarian, P., Gahinet, P., & Becker, G. (1995). Self-scheduled hinfinity control of linear parameter-varying systems: a design example. *Automatica*, *31*(9), 1251–1261.

Bai, E., & Giri, F. (2010). *Lecture notes in control and information sciences*: *Vol. 404. Block-oriented nonlinear system identification*. Berlin, Heidelberg: Springer.

Bruzelius, F., & Breitholtz, C. (2001). Gain scheduling via affine linear parameter-varying systems and H_∞ synthesis. In *IEEE conference on decision and control* (pp. 2386–2391).

Chesi, G., Garulli, A., Tesi, A., & Vicino, A. (2007). Robust stability of time-varying polytopic systems via parameter-dependent homogeneous lyapunov functions. *Automatica*, *43*, 309–316.

De Caigny, J., Camino, J. F., & Swevers, J. (2011). Interpolation-based modeling of MIMO LPV systems. *IEEE Transactions on Control Systems Technology*, *19*, 46–63.

Ferranti, F., Knockaert, L., & Dhaene, T. (2011). Passivity-preserving parametric macromodeling by means of scaled and shifted state-space systems. *IEEE Transactions on Microwave Theory and Techniques*, *59*, 2394–2403.

Goos, J., Lataire, J., & Pintelon, R. (2014). Estimation of linear parameter-varying affine state space models using synchronized periodic input and scheduling signals. In *American control conference* (pp. 3754–3759). Portland, OR, June.

Goos, J., Lataire, J., & Pintelon, R. (2015). Estimation of affine LPV state space models in the frequency domain: extension to transient behavior and non-periodic inputs. In *European control conference* (pp. 818–823). Linz, Austria, July.

Goos, J., & Pintelon, R. (2016). Minimal state space realization of continuous-time linear time-variant input–output models. *International Journal of Control*, *89*(4), 722–730.

Lataire, J., Louarroudi, E., & Pintelon, R. (2012). Detecting a time-varying behavior in frequency response function measurements. *IEEE Transactions on Instrumentation and Measurement*, *61*(8), 2132–2143.

Lataire, J., & Pintelon, R. (2011). Frequency domain weighted nonlinear least squares estimation of continuous-time, time-varying systems. *IET Control Theory & Applications*, *5*(7), 923–933.

Laurain, V., Tóth, R., Gilson, M., & Garnier, H. (2010). Direct identification of continuous-time linear parameter-varying input/output models. *IET Control Theory & Applications*, *5*(7), 878–888.

Laurain, V., Tóth, R., Zheng, W., & Gilson, M. (2012). Nonparametric identification of LPV models under general noise conditions: an LS-SVM based approach. In *Proc. of the 16th IFAC symposium on system identification* (pp. 1761–1766). Brussels, Belgium.
Lee, L. H., & Poolla, K. (1999). Identification of linear parameter-varying systems using non-linear programming. *Journal of Dynamic Systems*, *121*(1), 71–78.
Levine, W. S. (2011). *The control handbook—advanced methods of control. Vol. III* (2nd ed.). CRC Press.
Louarroudi, E., Lataire, J., Pintelon, R., Janssens, P., & Swevers, J. (2014). Parametric estimation of the evolution of the time-varying dynamics of periodically time-varying systems from noisy input–output observations. *Mechanical Systems and Signal Processing*, *47*, 151–174.
Mahata, K., Pintelon, R., & Schoukens, J. (2006). On parameter estimation using non-parametric noise models. *IEEE Transactions on Automatic Control*, *51*(10), 1602–1612.
Pintelon, R., Louarroudi, E., & Lataire, J. (2012). Detection and quantification of the influence of time variation in frequency response function measurements using arbitrary excitations. *IEEE Transactions on Instrumentation and Measurement*, *61*(12), 3387–3395.
Pintelon, R., & Schoukens, J. (2012). *System identification: a frequency domain approach* (2nd ed.). Wiley-IEEE Press.
Pintelon, R., Vandersteen, G., Schoukens, J., & Rolain, Y. (2011). Improved (non-) parametric identification of dynamic systems excited by periodic signals—the multivariate case. *Mechanical Systems and Signal Processing*, *25*(8), 2892–2922.
Rugh, W. J., & Shamma, J. S. (2000). Research on gain scheduling. *Automatica*, *36*(10), 1401–1425.
Scherer, C. (1996). Mixed H_2/H_∞ control for time-varying and linear parametrically-varying systems. *International Journal of Robust and Non-linear Control*, *6*, 929–952.
Tóth, R. (2010). *Modeling and identification of linear parameter-varying systems*. Heidelberg, Germany: Springer.
Tóth, R., Laurain, V., Gilson, M., & Garnier, H. (2012). Instrumental variable scheme for closed-loop LPV model identification. *Automatica*, *48*, 2314–2320.
Wiberg, D. (1971). *Schaum's outline series, State space and linear systems*. New York, USA: McGraw-Hill.
Wills, A., & Ninness, B. (2008). On gradient-based search for multivariable system estimates. *IEEE Transactions on Automatic Control*, *53*, 298–306.
Wu, F., & Dong, K. (2006). Gain-scheduling control of LFT systems using parameter-dependent Lyapunov functions. *Automatica*, *42*(1), 39–50.

Jan Goos was born in Geel (Belgium) in 1986. He graduated from the Katholieke Universiteit Leuven as an engineer in computer sciences (artificial intelligence) in 2009 and in mathematical engineering in 2011. In March 2016, he obtained a Ph.D. from the Department of ELEC at the Vrije Universiteit Brussel (VUB), under the guidance of Rik Pintelon.

His main interests are the modeling, measurement and identification of Linear Parameter Varying (LPV) systems, but he also loves non-linear dynamics.

Rik Pintelon was born in Gent, Belgium, on December 4, 1959. He received a master's degree in electrical engineering in 1982, a doctorate (Ph.D.) in engineering in 1988, and the qualification to teach at university level (geaggregeerde voor het hoger onderwijs) in 1994, all from the Vrije Universiteit Brussel (VUB), Brussels, Belgium. In 2014, he received the degree of Doctor of Science (D.Sc.) from the University of Warwick (UK) for publications with the collective title "Frequency Domain System Identification: A Mature Modeling Tool".

From 1982 to 1984 and 1986 to 2000, Dr. Pintelon was a researcher with the Belgian National Fund for Scientific Research (FWO-Vlaanderen) at the Electrical Engineering (ELEC) Department of the VUB. From 1984 to 1986, he did his military service overseas in Tunesia at the Institut National Agronomique de Tunis. From 1991 to 2000, he was a part-time lecturer in the Department of ELEC of the VUB, and since 2000 he is a full-time professor in electrical engineering at the same department. Since 2009 he is a visiting professor in the Department of Computer Sciences of the Katholieke Universiteit Leuven, and since 2013 he is a honorary professor in the School of Engineering of the University of Warwick.

His main research interests include system identification, signal processing, and measurement techniques. Dr. Pintelon is the coauthor of four books on system identification and the coauthor of more than 200 articles in refereed international journals. He has been a Fellow of IEEE since 1998. Dr. Pintelon was the recipient of the 2012 IEEE Joseph F. Keithley Award in Instrumentation and Measurement (IEEE Technical Field Award). He received the 2008 IOP outstanding paper award (best paper in Measurement Science & Technology), the 2014 Martin Black prize (best paper in Physiological Measurement) and the 2014 Andy Chi award (best paper in IEEE Trans. on Instrumentation and Measurement).